THE GRAVO-THERMAL CATASTROPHE IN ISOTHERMAL SPHERES AND THE ONSET OF RED-GIANT STRUCTURE FOR STELLAR SYSTEMS

D. Lynden-Bell and Roger Wood

(Communicated by the Astronomer Royal)

(Received 1967 August 1)

Summary

Self-gravitating systems have negative specific heats, thus if heat is allowed to flow between two of them, the hotter one loses heat and gets yet hotter while the colder gains heat and gets yet colder. Evolution is thus away from equilibrium. When a single isothermal sphere within a non-conducting box is sufficiently centrally condensed a similar instability arises between the central parts and the outer parts; as a result no equilibrium states exist for an isothermal sphere of energy E (<0) and mass M within a spherical box of radius greater than $0.335 \, GM^2/(-E)$. This is Antonov's discovery that no state of locally maximal entropy exists for stellar systems of given energy and mass contained within a rigid sphere of radius larger than this. The instability is distinct from that found by Ebert which is similar to the Schönberg–Chandrasekhar limit in stars and relates to isothermal spheres at fixed temperature. In fact there are four distinct critical points for instability of isothermal spheres which are related to the turning points of the four total thermodynamic free energies by Poincaré's theory of linear series of equilibria.

This study of the thermodynamics of self-gravitating spheres gives insight on the evolution and the final fate of stellar systems. It also helps in the understanding of some well known phenomena in stellar evolution. It is emphasized that these results prove that the escape of stars from a cluster is not necessary for its evolution but rather that extended systems naturally grow a core–halo structure reminiscent of the internal constitution of a red-giant star.

1. *Introduction.* This paper includes a thorough discussion of the thermodynamics of bounded self-gravitating isothermal spheres. Interest in this ancient subject arose as follows: work by Henon (**1**), (**2**) and numerical experiments by Aarseth (**3**) indicate that a stellar system sometimes forms a small dense nucleus which is to some extent independent of the outer parts of the system. Antonov's discussion of the entropy of isothermal systems (**4**) shows that their thermodynamics is strange and that evolution of very concentrated systems is not towards the isothermal sphere. This work aims to connect these facts by showing that the thermodynamics of concentrated systems makes them evolve into core–halo structures.

The work of Woolley (**5**)–(**7**), Michie (**8**), (**9**) and King (**10**), who have assumed approach to the isothermal structure, will need modification only at the very high central concentrations. King already noticed an anomaly in his models for this range.

To understand the strange thermodynamics brought to light by Antonov's discussion of the entropy, we have imagined our self-gravitating sphere to be

in the laboratory and have calculated theoretically the results of imaginary experiments conducted on it.

By such discussions we gain some insight into such problems as the final fate of stellar systems and the creation of their nuclei. In view of this intended application we are particularly interested in thermally isolated and even in completely isolated systems. As a consequence our work contrasts with the beautiful results of Ebert (11), (12) amplified by Bonner (13) and McCrea (14) in which gas spheres are under a given surface pressure and in thermal equilibrium with an external heat bath.

2. *An experiment* (*Antonov's problem*). A large number N of mass points (stars) of mass m were released under their mutual gravity inside a perfectly reflecting sphere off which they bounced with impunity. Their total energy was $E (< 0)$, their total mass $Nm = M$ and the radius of the sphere was r_e. Except for certain special initial conditions explained below we found that the system settled down to an equilibrium when r_e was less than the critical radius

$$r_c = 0.335 \, GM^2/(-E).$$

When r_e was larger than this the centre seemed to condense out and evolved towards very high temperatures and densities; no equilibrium state was attained. The temperature of the outer parts increased alarmingly but even so it was unable to catch up with the runaway temperature of the central nucleus. Entropy was continuously generated by heat conduction outwards from the nucleus. In an attempt to halt this runaway we reduced the radius of the box to slightly less than the critical radius, but to our surprise we found this of no avail. Far from returning to a more normal density the nucleus continued to condense and to get hotter at its own ever accelerating rate. The high temperatures were by now generating such pressure inside the box that we feared lest it burst. To relieve the pressure we expanded the box but found that this was only a temporary solution for the nucleus continued to get smaller and hotter and to supply heat to the outside at an alarming rate. Realizing that it was this heat flux which was the ultimate cause of the increased pressure on the box, we decided that we must at all costs reverse this flux. Since our sphere was non-conducting this could only be done by the dangerous procedure of pressing the sphere down to a much smaller radius. With much exterior reinforcement the sphere withstood the high temperatures involved, but we had to force it a long way inwards against enormous pressures before bringing the system under control. Only when we succeeded in reducing the box to a size less than some thirty times the much reduced radius of the nucleus, did we manage to raise the temperature of the outside above that of the nucleus and so reverse the heat flux. The systems then settled into a high temperature equilibrium. The radius was considerably smaller, the entropy much greater and the binding energy much less in this state than they were initially.

In further experiments we found that even for $r_e < r_c$ initial conditions in which a subgroup of the stars was tightly bound together by its own gravity did not lead to an equilibrium but rather to a runaway similar to that described above.

2.1 *Physical explanation*. For an isolated system at equilibrium in the absence of a wall the Virial theorem reads

$$2\mathcal{T} + \mathcal{V} = \mathcal{T} + E = 0, \qquad \text{i.e.} \quad \mathcal{T} = -E.$$

For such systems increase in E causes a decrease in the kinetic energy $\mathscr{T}$ and therefore in the kinetic energy per particle or temperature. Such systems have negative specific heats. It will not surprise the reader to learn that small modifications of the strict conditions of the Virial theorem do not modify this result and isothermal spheres within boxes also display negative specific heats provided the system is sufficiently centrally condensed; that is provided it can be regarded as mainly held in by its own gravity rather than by the pressure of the walls of the box. This condition is satisfied by isothermal spheres at radii considerably smaller than r_c (see Section 5).

Consider then the conditions of our exciting experiment. We start with our sphere in equilibrium in a box with $r_e < r_c$, we surround it with a box of radius greater than r_c and suddenly remove the inner box. (The system still has the same mass and energy so r_c remains unchanged.) The first readjustment made by the body to this sudden change is an expansion which causes some adiabatic cooling. All parts of the body expand because some pressure has been taken off the outside. However, the central parts which were always mainly held together by self-gravity do not expand as much as the outer parts which are only held in by wall pressure. As a result of this difference in expansion the central parts cool less than the outer parts so a temperature gradient is set up. With the gross conditions of hydrostatic support satisfied our attention turns to the slower thermal conduction processes. The heat flow is always down the temperature gradient so the heat flux is outwards. The inner parts being nearly self-gravitating have negative specific heat; thus as they lose the heat they shrink and grow hotter. The outer parts are held in by the walls and have positive specific heat. On receiving the heat they also grow hotter. It is now a race; if the outer parts have a specific heat smaller than the magnitude of the negative specific heat of the inner parts then the outer temperature will increase faster than the inner one. It will therefore catch up and a possible equilibrium state will be achieved. If however the outer parts are too extensive their specific heat will be large. Conductive transfer of heat from the central parts will then raise the high central temperature faster than it raises the lower temperature of the outer parts. This is what we call the gravo-thermal catastrophe. Now no equilibrium is possible; the centre continues to contract and get hotter giving out heat to the outer parts but the temperature difference increases and drives the evolution onwards still faster.

Detailed explanation of the rest of the experiment is best made with the help of the figures derived in the mathematical section.

In Fig. 2 we plot the dimensionless quantity $-Er_e/GM^2$ against a parameter $|v_1|$ which is the natural logarithm of the ratio of the central density of the configuration to that at the edge. The solid line then represents the locus of possible equilibrium states. Also in this diagram we indicate behaviour of the entropy for both equilibrium and non-equilibrium states. For a given energy and radius it is seen that the entropy is maximal for the equilibrium states up to the first hump of the curve (indicating that these states are stable). At the top the entropy curve has an inflection and states on the downward sloping portion of the curve have minimum entropy for given E, r_e (indicating unstable equilibrium).

In our experiment so far we have traversed the equilibrium series at constant E by increasing r_e as described. However when we reach the maximum A and increase the radius further so that $-Er_e/GM^2$ increases we move to a point such as B. As before the system tends to evolve spontaneously towards a state with

higher entropy but, unlike previous occasions, this time there is no local entropy maximum to which it can go and we have the runaway described above, with the entropy continuously increasing.

The compression of the box to below the critical radius involves both changes in E and r_e as well as in $|v_1|$. We, therefore, add a third dimension, log r_e, to our diagram and plot a *surface* on which equilibria are possible. We show a portion of the surface in Fig. 3. Since it would be confusing to draw in the entropy surfaces in the diagram we only plot the intersection of such surfaces with the equilibrium surface. The regions of high and low entropy on this surface are indicated. The first part of the experiment, increasing r_e at fixed E and M is now represented by the dotted line and the entropy is again seen to increase as far as P. Further expansion of the box increases both $-Er_e/GM^2$ and log r_e and so the configuration is specified by a point such as Q just above the equilibrium surface. We now have a situation identical to that at point B in Fig. 2 and a runaway ensues. All changes of configuration that do not take place on the equilibrium surface are indicated by solid lines.

It is now apparent that the system is going to higher and higher $|v_1|$ along a line that crosses surfaces of higher and higher entropy. These entropy surfaces only intersect the equilibrium surface at much lower values of r_e than the system has at present. To restore equilibrium, therefore, we must compress the box enough for an equilibrium state to be consistent with the present entropy. We can now see why our action of compressing the box below the old critical radius, and the expansion of the box to relieve the pressure, could not bring about a new equilibrium; the entropy was too high for the states so attained.

In our final drastic compression all three parameters plotted in Fig. 3 are decreased; (i) r_e is decreased; (ii) $-Er_e/GM^2$ is decreased both because of (i) and because by adding energy we decrease $-E$. (iii) $|v_1|$ is decreased because we are reducing the density contrast between the centre and the edge. Since the box is non-conducting the compression is at constant or spontaneously increasing entropy. At each stage a section through the equilibrium surface at a particular r_e would look like Fig. 1 and the system would be at a point such as C. This is unstable for the same reason that B was, so leaving the system near C would merely lead to further runaway. The compression continues until we arrive at a point, such as D, underneath the equilibrium surface where the entropy surfaces slope the other way so that spontaneous evolution decreases $|v_1|$. Evolution then continues spontaneously until entropy is maximized on the stable branch of the equilibrium surface.

2.2 *Other experiments.* In the experiment described above we investigated the stability of a self-gravitating system of fixed mass M, thermally isolated from its surroundings, and having the energy, E, and volume V, specified. At equilibria the entropy, S, is a maximum for given E and V. When discussing the stability of such systems for different external conditions it is natural to think in terms of the free energies. In the case of pressure equilibrium (i.e. a situation in which our rigid non-conducting wall is replaced by a perfectly plastic one, free to expand or contract under any pressure difference between the system and the constant pressure of the surroundings, but still non-conducting) the equilibria are states of maximum entropy for given *enthalpy* $\mathcal{H}$ and pressure P. Similarly, for a system surrounded by a perfectly conducting wall and in thermal equilibrium with its

surroundings (assumed to be a constant temperature heat bath) we can again consider cases where we have a rigid wall (fixing the volume) or a plastic wall (fixing the pressure); the free energies concerned are then the Helmholtz free energy, $\mathscr{F}$, and the Gibb's free energy, $\mathscr{G}$, respectively. A study of the behaviour of these free energies enables us to predict the results of experiments under the different conditions.

3. *The mathematical problem.* Equilibrium states in the presence of encounters are states of stationary entropy at given energy and volume. Here we study the problem of finding these. Taking Boltzmann's view of entropy we put

$$S = -k \sum_i \int f^i \log f^i d^6\tau \qquad (1)$$

where (i) S is the entropy,

(ii) k is Boltzmann's constant,

(iii) The integration is over the phase space available, that is over all velocities and over all positions within the confining sphere of radius r_e.

(iv) We have not assumed that all stars are of the same mass but have divided them into groups according to mass. f^i is the number density in phase space of stars of the ith group. f^i is a function of position in phase space. m^i is the average mass of a star in the ith group.

(v) Points in phase space will be specified by position vectors $\mathbf{r} = (x, y, z)$ and velocity vectors $\mathbf{c} = (u, v, w)$. We denote phase space integrations by the symbol

$$d^6\tau = d^3r\, d^3c = dxdydz\, dudvdw.$$

The states for which S is stationary subject to constraints are equilibria. The constraints are that the energy is fixed at E and that the numbers of stars in the different mass groups are fixed. If one wishes to consider rotating systems one must fix the total angular momentum $\mathbf{H}$. This is simple to do but the extra formal complication obscures our main point so we shall not do it here. Fixing $\mathbf{H} = 0$ gives the same result as ignoring the angular momentum altogether in the statistical calculations.

We define the total phase space density at $\mathbf{r}$, $\mathbf{c}$ to be $f(\mathbf{r}, \mathbf{c}) \equiv \sum_i m^i f^i(\mathbf{r}, \mathbf{c})$. The spatial density $\rho(\mathbf{r})$ is then

$$\rho(\mathbf{r}) = \int f(\mathbf{r}, \mathbf{c}) d^3c$$

with the integration over all velocities.

The kinetic energy is

$$\mathscr{T} = \sum_i \int \tfrac{1}{2} m^i c^2 f^i(\mathbf{r}, \mathbf{c}) d^6\tau = \int \tfrac{1}{2} c^2 f d^6\tau.$$

The total potential energy is $\mathcal{U}$

$$\mathcal{U} = -\frac{G}{2} \int\int \frac{\rho(\mathbf{r})\, \rho(\mathbf{r}')}{|\mathbf{r} - \mathbf{r}'|}\, d^3r\, d^3r'$$

which can alternatively be written

$$U = -\frac{G}{2} \int\int \frac{ff'}{|\mathbf{r}-\mathbf{r}'|} \, d^6\tau \, d^6\tau'$$

where $f' = f(\mathbf{r}', \mathbf{c}')$.

Thus the total energy E

$$E = \mathscr{T} + U = \int \tfrac{1}{2}c^2 f \, d^6\tau - \frac{G}{2} \int\int \frac{ff'}{|\mathbf{r}-\mathbf{r}'|} \, d^6\tau \, d^6\tau'. \tag{2}$$

The total number of stars in the ith mass group is

$$N^i = \int f^i \, d^6\tau. \tag{3}$$

Our problem is to maximize the entropy S, given by (1), keeping the energy E, (2), and the numbers N^i, (3), constant. We do this using Lagrange multipliers $k\beta'$ and $k\alpha^i$

$$\delta S = \delta S + k\beta' \delta E + \sum_i k\alpha^i \delta N^i$$

$$= \left\{ \begin{array}{l} -k\sum_i \int \delta f^i (\log f^i + 1) \, d^6\tau \\[2mm] +k\beta' \left[\int \tfrac{1}{2}c^2 \delta f d^6\tau - \frac{G}{2} \int\int \frac{f\delta f' + \delta ff'}{|\mathbf{r}-\mathbf{r}'|} \, d^6\tau \, d^6\tau' \right] \\[2mm] +\sum_i k\alpha^i \int \delta f^i \, d^6\tau. \end{array} \right\} \tag{4}$$

By exchanging the dummy variables $\mathbf{r}, \mathbf{c}$ and $\mathbf{r}', \mathbf{c}'$ in the $f \delta f'$ term of the potential energy contribution, we see that on integration this term is equal to the $f' \delta f$ terms so δE may be written

$$\delta E = \int \delta f \left[\tfrac{1}{2} c^2 - G \int \frac{f'}{|\mathbf{r}-\mathbf{r}'|} \, d^6\tau' \right] d^6\tau,$$

$$\delta E = \int \left(\sum_i m^i \, \delta f^i \right) (\tfrac{1}{2} c^2 - \psi(\mathbf{r})) \, d^6\tau \tag{5}$$

where $\psi(\mathbf{r})$ is the gravitational potential caused by the density corresponding to f, i.e.

$$\psi(\mathbf{r}) = G \int \frac{\rho(\mathbf{r}')}{|\mathbf{r}-\mathbf{r}'|} \, d^3\mathbf{r}' = G \int \frac{f(\mathbf{r}', \mathbf{c}')}{|\mathbf{r}-\mathbf{r}'|} \, d^6\tau'. \tag{6}$$

Substituting the expression (5) for the δE term in equation (4)

$$\delta S = -k\sum_i \int \delta f^i \left[\log f^i + 1 + \beta' m^i \left(\frac{c^2}{2} - \psi \right) + \alpha^i \right] d^6\tau.$$

Since the δf^i may now be considered independent within the integration the condition that S should be stationary ($dS = 0$) gives

$$\log f^i + 1 + \beta' m^i \left(\frac{c^2}{2} - \psi \right) + \alpha^i = 0.$$

$$f^i = A^i e^{-\beta' \epsilon^i} = A^i e^{-\beta' m^i \epsilon} \tag{7}$$

where

$$\epsilon^i = m^i \left(\frac{c^2}{2} - \psi\right), \qquad \epsilon = \frac{c^2}{2} - \psi \tag{8}$$

and

$$A^i = \exp\left[-(\alpha^i + 1)\right].$$

As expected equation (7) is the Maxwell–Boltzmann distribution and we note from equations (8) and (6) that it is Maxwell–Boltzmann within the self-consistent potential $\psi(\mathbf{r})$.

We now show that equation (7) gives equipartition of kinetic energy for the average star of each type for all positions. The average kinetic energy of a star of mass m^i at $\mathbf{r}$ is

$$\frac{\int f^i(\mathbf{r}, \mathbf{c})\, m^i \frac{c^2}{2}\, d^3c}{\int f^i(\mathbf{r}, \mathbf{c})\, d^3c} = \frac{\int \exp\left(-\beta' m^i \frac{c^2}{2}\right) m^i \frac{c^2}{2}\, d^3c}{\int \exp\left(-\beta' m^i \frac{c^2}{2}\right) d^3c} = \frac{3}{2\beta'}, \tag{9}$$

which is independent of both i and $\mathbf{r}$ as required. This also indicates that β' should be identified with $1/kT$ where T is the temperature. We show in Appendix I that β' is indeed an integrating factor for the heat and so gives an absolute thermodynamic temperature.

Although equation (7) is in part the solution to the stationary entropy problem nevertheless $\psi(\mathbf{r})$ appears implicitly in its right hand side. ψ itself was defined by equation (6) which involves f again (and therefore f^i). The procedure to break this roundabout is to integrate equation (7) to obtain an equation for ψ, solve it, and substitute the solution back in equation (7) to obtain the explicit solution for f^i.

Integrating equation (7) we obtain the density of the ith mass group

$$\rho^i = \int m^i f^i\, d^3c = B^i \exp(\beta' m^i \psi), \qquad r < r_e$$

where

$$B^i = A^i \left(\frac{2\pi}{m^i \beta'}\right)^{3/2} \tag{10}$$

and has the dimensions of density. The total density is

$$\rho = \sum_i \rho^i = \sum_i B^i \exp(\beta' m^i \psi), \qquad r < r_e$$

so the potential is

$$\psi(\mathbf{r}) = G \int_{r < r_e} \frac{\rho(\mathbf{r}')}{|\mathbf{r} - \mathbf{r}'|}\, d^3r' = G \int_{r' < r_e} \frac{\sum_i B^i \exp[\beta' m^i \psi(\mathbf{r}')]}{|\mathbf{r} - \mathbf{r}'|}\, d^3r'.$$

This integral equation for ψ may be solved by differentiation which gives

$$\nabla^2 \psi(\mathbf{r}) = -4\pi G \rho(\mathbf{r}) = \begin{cases} -4\pi G \sum B^i \exp(\beta' m^i \psi(\mathbf{r})), & r < r_e \\ 0 & r > r_e \end{cases} \tag{11}$$

This equation must be solved under the boundary condition that ψ is of order $1/r$ at infinity and ψ and $\partial\psi/\partial r$ are continuous at $r = r_e$.

In Appendix II we repeat Antonov's proof that only spherically symmetrical states can correspond to local entropy *maxima*. Thus only spherically symmetrical solutions need to be considered. To proceed further with the general case numerical integration of the ordinary differential equation is required. This presents no difficulties, but it is instructive to study the simple case of just one mass group in greater detail. We specialize in stars of one mass only and drop the suffix i. Equation (11) then reduces to the well known equation for the isothermal gas sphere.

$$\frac{1}{r^2} \frac{d}{dr} \left(r^2 \frac{d\psi}{dr} \right) = -4\pi GB \exp (\beta\psi), \qquad r < r_e \qquad (12)$$

where $\beta = m\beta'$.

It is well known that there are three classes of solutions to this equation:

(1) the singular solution

$$\psi = \frac{1}{\beta} \log [r^{-2} (2\pi G\beta B)^{-1}],$$

(2) the isothermal gas sphere solutions with finite density at $r = 0$,

(3) the general solutions whose densities tend to zero as r approaches zero. We have not as yet imposed any condition to determine the gravitational flux emanating from $r = 0$. Considering each type of solution in turn we find that no flux arises from $r = 0$ in solutions of type 1 and 2 but that all solutions of class 3 have a flux corresponding to a negative mass situated at the centre. We reject such unphysical solutions and find later that the singular solution is in fact the limiting case of the finite density solutions. These therefore become our main concern. We have not, as has been customary, rejected infinite density solutions but we have shown that the only one that can exist is the singular solution 1.

The transformation

$$\left. \begin{aligned} v_1 &= \beta(\psi - \psi(0)) \\ r_1 &= \{4\pi G\beta B \exp [\psi(0)\beta]\}^{1/2} r \\ &= (4\pi G\rho_0\beta)^{1/2} r \end{aligned} \right\} \qquad (13)$$

is applicable to solutions of class 2 provided $\psi(0)$ is finite. Note that we may then write the density in the form

$$\rho = \rho_0 e^{v_1} \qquad (14)$$

Equation (12) reduces to the standard Emden form **(15)**

$$\frac{d^2 v_1}{dr_1^2} + \frac{2}{r_1} \frac{dv_1}{dr_1} + e^{v_1} = 0 \qquad (15)$$

(the variables are named differently by Chandrasekhar (**16**)). The solutions of class 2 when transformed all become the standard solution of equation (15) for which

$$v_1 = \frac{dv_1}{dr_1} = 0$$

when $r_1 = 0$. However these solutions are terminated by the box at different radii given by $r_1 = \{4\pi G\rho_0\beta\}^{1/2} r_e$. The solution is readily computed numerically

and was tabulated by Emden. With the solutions known it is possible to calculate the total energy and total mass within r_e, and to choose the values of β, B etc. so that the energy is E and the mass M. We may also calculate the total entropy S, the surface pressure p etc. So far this section has merely rederived well known results which are all too depressingly familiar and must have been derived some hundreds if not thousands of times before. However, it is at this point that Antonov asked and answered the crucial question: are these configurations of stationary entropy genuine entropy maxima or are they saddle points, inflection points, etc.? He also distinguished carefully the case of a local entropy maximum, in which the configuration has more entropy than all *neighbouring* configurations of the same mass and energy inside the same sphere, and global entropy maxima for which the other configurations are not necessarily neighbouring.

In Appendix III we give Antonov's demonstration that no globally maximum entropy state exists for particles of fixed total energy inside a box of fixed radius. He also showed that locally maximum entropy states only exist provided the radius of the box is less than $0 \cdot 335 \ GM^2/-E$. This corresponds to a density contrast between the centre and the edge of the confined isothermal sphere of a factor 709. We shall find these results among others in our study of the series of equilibria of the bounded isothermal gas sphere. Antonov's method was a more direct study of the second order terms in the variation of the entropy at constant energy, mass and confining radius.

3.1 *Calculation of thermodynamic parameters for bounded isothermal spheres.* Certain relationships between thermodynamic variables follow without use of detailed structure computations. In this section we first deduce such relationships and then show how Emden's tables or their equivalent may be used to deduce the values of all variables.

The virial theorem of Clausius may be applied to our equilibrium system provided the surface pressure terms are not dropped. For an equilibrium it reads

$$2\mathscr{T} + \mathcal{U} = 3pV \tag{16}$$

where p is the surface pressure

$$p = \int f^1 \tfrac{1}{3} mc^2 d^3c |_{r_e} \tag{17}$$

$$V = \tfrac{4}{3}\pi r_e{}^3 \text{ is the volume} \tag{18}$$

$\mathcal{U}$ is the total potential energy

$\mathscr{T}$ is the total kinetic energy.

From our equipartition theorem we have

$$\mathscr{T} = \frac{3}{2}\frac{M}{m\beta'} = \frac{3}{2}\frac{M}{\beta} \tag{19}$$

while the definition of total energy reads

$$E = \mathscr{T} + \mathcal{U}$$

so using the Virial theorem

$$E = 3pV - \mathscr{T} = 3pV - \frac{3}{2}\frac{M}{\beta}; \tag{20}$$

similarly

$$U = 3pV - 3\frac{M}{\beta} \qquad (21)$$

which vanishes for a perfect gas in the absence of gravitation as it should. The surface pressure may be related to the edge density by use of the equipartition theorem

$$p = \int_{\text{at } r_e} f^1 \tfrac{1}{3} mc^2 d^3c = \tfrac{2}{3}\frac{3}{2\beta'} \int_{\text{at } r_e} f^1 d^3c = \frac{\rho_e}{m\beta'} = \frac{\rho_e}{\beta}. \qquad (22)$$

For one mass group equation (7) takes the form

$$f^1 = A \exp\left[-\beta\left(\frac{c^2}{2} - \psi\right)\right] \qquad (23)$$

and at $r = r_e$

$$\psi = \frac{GM}{r_e}$$

so

$$\frac{\rho_e}{m} = \int A \exp\left[-\beta\left(\frac{c^2}{2} - \frac{GM}{r_e}\right)\right] d^3c = A\left(\frac{2\pi}{\beta}\right)^{3/2} \exp\left(\beta\frac{GM}{r_e}\right). \qquad (24)$$

Relationships (16)–(24) enable us to simplify our expression for the entropy into the form given by equation (25) as follows:

$$S = -k\int f^1 \log f^1 d^6\tau = -k\left[\int f^1 \log A\, d^6\tau - \int f^1 \beta\frac{c^2}{2} d^6\tau + \beta\int f^1 \psi\, d^6\tau\right]$$

hence

$$\frac{S}{k} = -\frac{M}{m}\log A + \beta'\mathcal{T} - \beta'\int \rho\psi\, d^3r. \qquad (25)$$

A is eliminated in favour of p by use of equations (24) and (22) to give

$$\frac{S}{k} = -\frac{M}{m}\log(p\beta'^{5/2}) + \beta'\left(\frac{GM^2}{r_e} + \mathcal{T} + 2U\right) - \frac{3}{2}\frac{M}{m}(\log m)$$

$$= -\frac{M}{m}\log(p\beta'^{5/2}) + \beta'\left(\frac{GM^2}{r_e} + 2E\right) - \frac{3}{2}\frac{M}{m}(1 + \log m). \qquad (26)$$

Alternatively we may use β instead of β' to obtain the form

$$\frac{mS}{k} = -M\log(p\beta^{5/2}) + \beta\left(\frac{GM^2}{r_e} + 2E\right) - \frac{3}{2}M(1 - \frac{2}{3}\log m). \qquad (27)$$

Further relationships require use of the solution to the isothermal equation (15). Emden gives the functions $v_1(r_1)$ etc. in his tables so we express our thermodynamic functions in terms of these dimensionless variables. We place stress on the functions $r_1^2 e^{v_1}$ and $-r_1 v_1'$ both of which become constant for large r_1 oscillating as they do so.

Radius. By definition equation (13):

$$r_1 = (4\pi G \rho_0 \beta)^{1/2} r.$$

The value of r_1 at the edge $r = r_e$ deserves a name; we call it z. It is the dimensionless radius out to which the isothermal sphere extends before it reaches the box.

It is a non-linear monotonic function of the density contrast between centre and edge. Actually

$$\frac{\rho}{\rho_0} = \exp v_1(z),$$

$v_1(r_1)$ decreases monotonically from zero at $r_1 = 0$.

By its definition

$$z = (4\pi G \, \rho_0 \beta)^{1/2} \, r_e \tag{28}$$

Mass

and

Temperature

so

$$GM = -\left(r^2 \frac{d\psi}{dr}\right)_{r_e} = -\frac{r_e}{\beta}\left(r_1 \frac{dv_1(r_1)}{dr_1}\right)_z,$$

$$\frac{GM\beta}{r_e} = -zv_1'. \tag{29}$$

Here and hereafter v_1, v_1' are understood to mean $v_1(z)$ and $v_1'(z)$ respectively. $GM\beta/r_e$ is plotted against the central concentration $|v_1|$ in Fig. 1.

Pressure. Formulae (14) and (22) read

$$\rho_e = \rho_0 \, e^{v_1}; \quad p = \frac{\rho_e}{\beta},$$

whence using equation (29) for β

$$p = \frac{z^2}{4\pi G\beta r_e^2} \cdot \frac{e^{v_1}}{\beta} = \frac{GM^2}{4\pi r_e^4} \cdot \frac{z^2 \, e^{v_1}}{(-zv_1')^2} \tag{30}$$

and so

$$3pV = \frac{GM^2}{r_e} \cdot \frac{z^2 \, e^{v_1}}{(-zv_1')^2}.$$

Energy. Returning to equation (20) for the energy and eliminating β by means of equation (29)

$$E = \frac{GM^2}{r_e}\left[\frac{z^2 \, e^{v_1}}{(-zv_1')^2} - \frac{3}{2}\frac{1}{(-zv_1')}\right]. \tag{31}$$

Entropy. Formulae (29)–(31) enable us to calculate the entropy in the form

$$\frac{mS}{kM} = \tfrac{1}{2}\log V - 2\log z - \tfrac{1}{2}\log(-zv_1') + (-zv_1')$$

$$-v_1 + \frac{2Er_e}{GM^2}(-zv_1') + \text{const.} \tag{32}$$

Constants may be omitted with impunity from the entropy, while Er_e/GM^2 is given as a function of z in equation (31) and plotted as a graph in Fig. 2. Likewise equations (18), (20) and (27)–(31) enable us to calculate other thermodynamic variables.

3.2 *Asymptotic forms for the thermodynamic variables.* We have pointed out that in general the solution of equation (15) must be computed numerically. However for large values of r_1 an analytic asymptotic form may be deduced as follows. Transform variables to

$$\theta = \log r_1, \qquad u = v_1 + 2\theta.$$

32

Equation (15) then becomes

$$\frac{d^2u}{d\theta^2}+\frac{du}{d\theta}+e^u-2 = 0.$$

This is the equation of a damped oscillator in the potential well e^u-2u. This well has a positive minimum at $u = \log 2$. Asymptotically the motion damps out and the oscillator comes to rest at the minimum so $u \to \log 2$ as $\theta \to \infty$. For those who prefer a more mathematical proof let us consider the energy Λ of the oscillator.

$$\Lambda = \frac{1}{2}\left(\frac{du}{d\theta}\right)^2+(e^u-2u)$$

and the oscillation equation may be written

$$\frac{d\Lambda}{d\theta} = -\left(\frac{du}{d\theta}\right)^2 \leqslant 0.$$

The energy always decreases but Λ as indicated above consists of two essentially positive terms. Hence $du/d\theta \to 0$ as $\theta \to \infty$. It then follows from the original equation that $u \to \log 2$ as $\theta \to \infty$.

Transforming again via

$$u_1 = u-\log 2,$$

the equation becomes

$$\frac{d^2u_1}{d\theta^2}+\frac{du_1}{d\theta}+2e^{u_1}-2 = 0.$$

For large θ, u_1 is small and expanding the exponential and taking only the first two terms we have

$$\frac{d^2u_1}{d\theta^2}+\frac{du_1}{d\theta}+2u_1 = 0.$$

A solution is

$$u_1 = Ae^{\lambda\theta}$$

where A, λ are constants. Solving for λ in the usual way and taking only the real part of the exponential we have for u_1

$$u_1 = Ae^{-\theta/2}\cos\left[\frac{\sqrt{7}}{2}(\theta+\alpha)\right]$$

Where α is some 'phase' constant.

Hence v_1 is

$$v_1 = \log 2-2\theta+Ae^{-\theta/2}\cos\left[\frac{\sqrt{7}}{2}(\theta+\alpha)\right]$$

and we can differentiate this to get

$$\frac{dv_1}{d\theta} = r_1\frac{dv_1}{dr_1}.$$

We note that $r_1{}^2e^{v_1} = e^{v_1+2\theta}$ is readily obtainable. Then with quantities v_1, $-r_1(dv_1/dr_1)$, $r_1{}^2e^{v_1}$, we can evaluate the asymptotic forms of all other thermodynamic variables as given in equations (29)–(32), e.g.

$$M = +\frac{r_e}{G\beta}\left\{2+\tfrac{1}{2}Ae^{-\theta/2}\cos\left[\frac{\sqrt{7}}{2}(\theta+\alpha)\right]+\frac{\sqrt{7}}{2}Ae^{-\theta/2}\sin\left[\frac{\sqrt{7}}{2}(\theta+\alpha)\right]\right\} \quad (33)$$

In particular we note that as $\theta \to \infty$

$$r_1{}^2 e^{v_1} \to 2; \quad -r_1 \frac{dv_1}{dr_1} \to 2,$$

so that

$$M \to \frac{2r_e}{G\beta},$$

$$p \to \frac{1}{2\pi G\beta^2 r_e{}^2},$$

and since $p = \dfrac{\rho}{\beta}$

$$\rho \to \frac{1}{2\pi G\beta r_e{}^2},$$

$$E \to -\frac{r_e}{G\beta^2},$$

$$\frac{m}{kM} S \to \log\left(2\pi G r_e{}^2\right) - \tfrac{1}{2} \log\left(\beta\right).$$

These expressions give the limiting behaviour of the thermodynamic variables as $\theta \to \infty$. We compare them with the results derived in the next section for the singular solution 1.

3.3 *The singular infinite density solution.* In the singular case the solution of equation (15) is

$$v_1 = \beta\psi = -2 \log r - \log\left(2\pi G B\beta\right).$$

But we know

$$\rho = Be^{v_1},$$

so that

$$\rho = \frac{1}{2\pi G\beta r^2},$$

giving

$$M(r) = \int_0^r 4\pi r^2 \rho\, dr = \frac{2r}{G\beta}.$$

We see at once that these last two results are identical to the corresponding limits of the last section. In fact it is found that the other thermodynamic variables, as given in equations (18)–(22) and (27) also give the limiting values found above. Thus the singular infinite density model is the limit of the family of finite density models as they become more centrally condensed.

4. *Stability.* In this section we reconsider the general theory of linear series of static equilibria, which is particularly suitable for discussing stability. We apply this approach to thermodynamic systems, with special reference to self-gravitating isothermal spheres subject to the different external conditions described in Section 2.2. As a preliminary to this general analysis we include a paragraph on the specific heat of these objects, since the sign of the specific heat is intimately connected with stability.

4.1 *Specific heat.* By definition the specific heat at constant volume is

$$C_V = \left(\frac{dE}{dT}\right)_{r_e} = k\left(\frac{dE}{d\left(\frac{1}{\beta}\right)}\right)_{r_e} = -k\beta^2\left(\frac{dE}{d\beta}\right)_{r_e} = -k\beta^2\frac{\left(\frac{dE}{dv_1}\right)_{r_e}}{\left(\frac{d\beta}{dv_1}\right)_{r_e}}. \tag{34}$$

If we consider a system of constant mass inside a fixed box then the variation of the inverse temperature β and the energy E with v_1 may be plotted using equations (29) and (31) and are shown as Figs 1 and 2 respectively. The sign of the specific
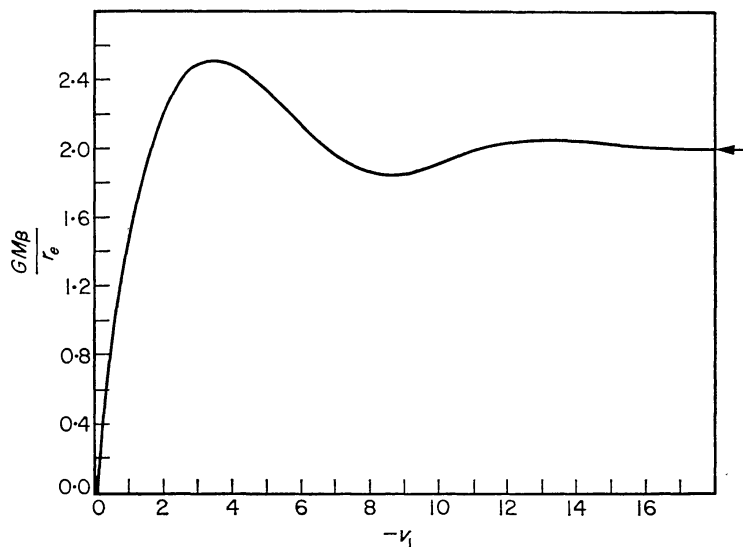

FIG. 1. *Radius–temperature–density contrast relationship.* $-v_1 = -\log\dfrac{\rho(z)}{\rho_0}$ *is a monotonic function of z. See Table and Ref.* (**15**).

heat for a particular configuration depends on the gradients of these two curves at the value of v_1 which specifies that configuration. It is seen that for small v_1 the specific heat is positive and that it increases until it becomes infinite at $v_1 = 3 \cdot 5$, the turning point of $(d\beta/dv_1)_{r_e}$. For v_1 just greater than this C_V is large and negative and remains negative for progressively larger values of v_1 until $v_1 = 6 \cdot 5$, the turning point of $(dE/dv_1)_{r_e}$, is reached, when it passes through zero to become positive again. The whole sequence is repeated for larger v_1. To relate this to the stability we consider Fig. 1, still thinking of M and r_e as fixed so that we have β as a function of v_1, and consider an equilibrium configuration at small v_1 in contact with a heat bath. As the temperature of the bath is decreased the central concentration starts by increasing but later becomes multivalued. For this latter portion of the temperature range several central concentrations are available for a single temperature. We see also that if the temperature is sufficiently decreased no equilibrium state exists at *any* concentration. The least temperature attainable by an equilibrium isothermal sphere of radius r_e and mass M is

$$T_{\min} = \frac{GmM}{2 \cdot 52\,kr_e}$$

and is achieved at $v_1 = 3 \cdot 5$ (or a density contrast, ρ_0/ρ, of $32 \cdot 2$). This is just the point at which C_V became negative and it is easy to see in physical terms why no equilibrium is possible for a system of negative specific heat in contact with

a heat bath. If the sphere is cooler than the bath it will accept heat from it and grow still cooler as a result, thus becoming unstable. Similarly if the sphere is hotter than the bath it loses heat and becomes hotter. We must be careful to note that both these instabilities depend on the presence of the heat bath; that thermally isolated systems do not suffer this type of instability* is illustrated in Fig. 2 where there is no turning point until $z = 34$, $v_1 = 6 \cdot 6$.

A similar instability is found at $v_1 = 2 \cdot 6$ by consideration of the specific heat at constant pressure, C_p, and this is the critical point discovered by Ebert. Since details of this instability are already in the literature we shall not discuss it further here but merely refer the reader to the relevant critical curve, Fig. 5.
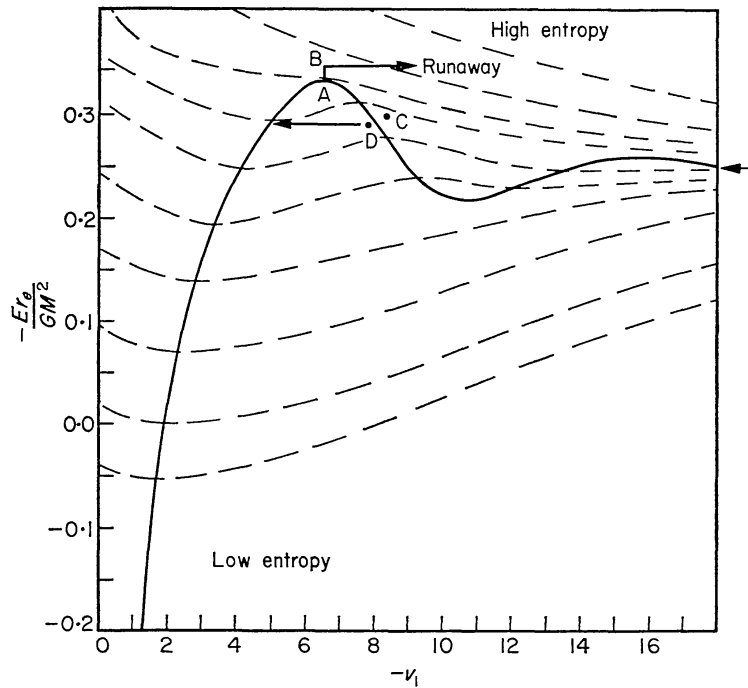

Fig. 2. *Energy–radius–density contrast relationship. By using v_1 as a coordinate we represent all spherical equilibria in the diagram. Other spherical displacements, corresponding to other generalized coordinates q_i, will therefore remain stable displacements along the sequence. The constant entropy lines are purely schematic; v_1 may be defined for the non-equilibrium configurations with densities*

$$\rho = \begin{cases} \rho_0 \exp v_1(r_1) & v_1(r_1) < v_1 \\ o & r > r_e. \end{cases}$$

but with non equilibrium energies E. The entropy of such a configuration falls below the equilibrium entropy for that v_1 and r_e by

$$\frac{3}{2} \frac{kM}{m} \log \left(\frac{E_0}{E}\right).$$

Here E_0 is the equilibrium's energy.

4.2 *Linear series of equilibria.* In statics the condition for a stable equilibrium is that the potential energy is a minimum. In many static problems the description

---

* In the thermodynamics of homogeneous equilibria negative specific heats always give rise to thermal instabilities between different parts of the system. This is not so here, where we have a grossly inhomogeneous equilibrium coupled together by the long range gravity field.

of the system depends on some parameter other than the generalized coordinates q_i in terms of which we describe the configuration of the system. An example of such a parameter would be the length of a lever arm or the fixed angular velocity at which a system is forced to spin. Such a parameter is a part of the definition of the system considered so the condition for a stable equilibrium takes the form $\mathcal{U}(\mu; q_i, \dots)$ is a local minimum for variations in the q_i keeping μ fixed at the prescribed value.

Let us call the value of q_i attained at such a local minimum q_i^0. These q_i^0 will depend on the specification of the problem so in particular if μ is changed to some different value the q_i^0 will be different in general. Thus we write

$$q_i^0 = q_i^0(\mu).$$

Furthermore the minimum value of $\mathcal{U}$ attained at any definite value of μ may be written

$$\mathcal{U} = \mathcal{U}(\mu; q_i^0(\mu), \dots).$$

Now let us plot the surfaces

$$\mathcal{U}(\mu; q_i, \dots) = \text{const} = \mathcal{U}_0 \text{ (say)}$$

in the multidimensional $(\mu, q_i \dots)$ space.

Each point corresponds to one configuration which has one potential energy so no two of the surfaces can intersect. Wherever one of these surfaces just touches one of the planes $\mu = \text{const}$ the configuration corresponding to the point of contact is an equilibrium since for fixed μ, $\mathcal{U}(\mu; q_i, \dots)$ is stationary there. Let us suppose that for some value $\mu = \mu_0$ we know that the system has a stable equilibrium. Then the point $q_i^0(\mu_0)$ is the tangent point of the surface $\mathcal{U} = \mathcal{U}_0$ and the plane $\mu = \mu_0$ and $\mathcal{U}_0$ is the minimum value that $\mathcal{U}$ attains in that neighbourhood of the plane. Note that one may also deduce that μ_0 is the extremal value of μ attained in that neighbourhood of the surface $\mathcal{U} = \mathcal{U}_0$. If the $\mathcal{U} = \mathcal{U}_0$ surfaces are concave towards the higher values of $\mathcal{U}$ in the neighbourhood of a tangent point then the configuration is stable. Furthermore concavities at touching points at neighbouring values of μ will normally be the same so that a whole linear series of stable equilibria may be traced out as μ is varied. It is shown in many classical works (**17**)–(**20**) that such a series of stable equilibria only terminate when it meets another series or turns back through the values of μ that it has already traversed. The reason behind this is topological and is most readily understood by drawing. The case we shall be concerned with here is that of a series of stable equilibria which is traversed as we change μ. The series turns back so that when we set μ above some critical value there is no equilibrium.

Although these concepts arose in classical statics they are very generally applicable throughout thermodynamics and dynamics. In dynamics gyroscopic terms appear which considerably complicate application of the method unless friction is also present but in thermodynamics the whole theory may be cast in similar form.

4.3 *Applications of linear series of equilibria in thermodynamics.* Consider our system of particles of total energy E inside a fixed spherical box of radius r_e. The condition of equilibrium is that $-S$ (the negative of the entropy) should be a minimum for fixed E. Thus $-S$ takes the place of $\mathcal{U}$ and E takes the place of μ.

The set of all coordinates q_i that specify the configuration is replaced by the distribution function $f(\mathbf{r}, \mathbf{c})$. We consider the sequence of equilibria of increasing E and we plot the sequences in E, v_1 space where $v_1 = \log_e(\rho_e/\rho_0)$ and ρ_e is the density at the edge. We have already shown that all spherical equilibrium configurations are Maxwellian and are included in Fig. 2.

At large positive E the system behaves like the non-gravitating gas sphere and the equilibria are stable. As E is decreased we traverse the equilibrium sequence of Fig. 2 and S steadily increases until the sequence turns back towards larger values of E. At the top we reach the maximum entropy attainable at equilibrium with box radius r_e. The entropy surfaces have an inflection here and, at this value of E, higher values of the entropy can be attained by moving off the equilibrium sequence to the right in Fig. 2. The sequence thus loses stability here. We remark again that the stable series is not only the series of states of maximum entropy for fixed energy but also the sequence of minimum energy for fixed entropy as may be seen from Fig. 2. We use this in Appendix II.
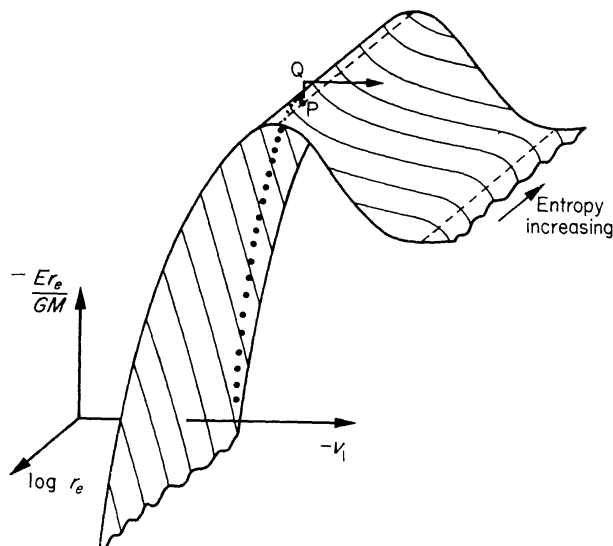

Fig. 3. *As Fig. 2 showing the equilibrium surface and its intersections with the constant entropy surfaces.*

Above we chose to discuss the series of equilibria at fixed r_e for E varying. We thus established that stable equilibria exist well into the range in which E is negative. However starting from any one of these stable configurations we could equally well discuss series at fixed E and varying r_e. The figure for the equilibrium sequence is precisely Fig. 2 but the positions of the constant entropy line are slightly altered because S depends on the volume of the box as well as on the density contrast. However even these constant entropy lines are qualitatively similar. To explain the situation more fully we have drawn the three dimensional diagram which plots the lines of constant entropy on the equilibrium surface in $(-Er_e/GM^2, v_1, \log r_e)$ space, Fig. 3. Since $-Er_e/GM^2$ is a function of v_1 alone this surface of states of equilibrium is cylindrical (in the general sense). However the surfaces of constant S are not cylindrical and intersect the equilibrium surface in the lines shown.

We have shown in detail how to determine the stable series of equilibria when our system is in a rigid box and exchanges no heat with the outside world. Basically

we used the fact that there was a functional $(-S)$ of the distribution function describing the system which was a minimum for certain fixed conditions. However starting from the law of entropy

$$TdS \geqslant dE + pdV$$

one can readily prove not only (i) below but also (ii), (iii) and (iv) below. As an example we prove (ii). For spontaneous change entropy increases so the inequality holds. We have

$$d\mathscr{F} = dE - TdS - SdT < -pdV - SdT.$$

For spontaneous changes at fixed V and T, $d\mathscr{F}$ must be negative. Now consider a point at which $\mathscr{F}$ is a minimum for given V and T. Then no change exists for which $d\mathscr{F}$ is negative so spontaneous changes can not occur. The system is therefore in stable equilibrium.

Similarly:

(i) for a system in stable equilibrium with fixed E and V the entropy S is a maximum $(-S$ is a minimum$)$;

(ii) for a system in stable equilibrium with fixed T and V the Helmholtz free energy $\mathscr{F} = E - TS$ is a minimum;

(iii) for a system in stable equilibrium with fixed entropy and pressure the enthalpy $\mathscr{H} = E + pV$ is a minimum. We shall use this in the variant form that S is a maximum at constant $\mathscr{H}$ and p;

(iv) for a system in stable equilibrium with fixed T and p the Gibbs free energy $\mathscr{G} = E - TS + pV$ is a minimum.

The graph of $GM\beta/r_e$ as a function of v_1 is shown in Fig. 1. Since β is a function of T and v_1 is a measure of r_e this is the sequence of equilibria envisaged in (ii) and we could mark values of $\mathscr{F}$ up the series. The series turns over at $z = 9$ and the minimum of $\mathscr{F}$ on the equilibrium sequence is attained there. For completeness we would need a three dimensional diagram like Fig. 3 but all these diagrams look alike and it is too time consuming to draw all of them. We deduce that stability ceases at this turnover point, following Section 2.1.

In Figs 4 and 5 we plot $\mathscr{H}/(pG^3M^6)^{1/4}$ against $|v_1|$ and $G^3M^2\beta^4p$ against $|v_1|$. These are combinations of the independent variables of (iii) and (iv) which are functions of v_1 alone. Namely

$$\mathscr{H}/(pG^3M^6)^{1/4} = \left[\tfrac{4}{3}z^2\,e^{v_1}(-zv_1')^{-2} - \tfrac{3}{2}(-zv_1')^{-1}\right]\left[\frac{(-zv_1')^2}{4\pi\,z^2e^{v_1}}\right]^{1/4}$$

and

$$G^3M^2\beta^4p = \frac{1}{4\pi}\,(z^2v_1')^2z^2e^{v_1}.$$

The maxima of these curves correspond to the least values of $-S$ and $\mathscr{G}$ attainable on such sequences of equilibria. Stability ceases at such points which are tabulated in Section 5.

4.4 *Adiabats and isotherms.* Although free energies are the most complete and powerful descriptions of thermodynamic systems nevertheless few physicists think in terms of the surfaces of constant free energy. By contrast adiabats and isotherms are familiar from the schoolroom cradle and are therefore more readily visualized.
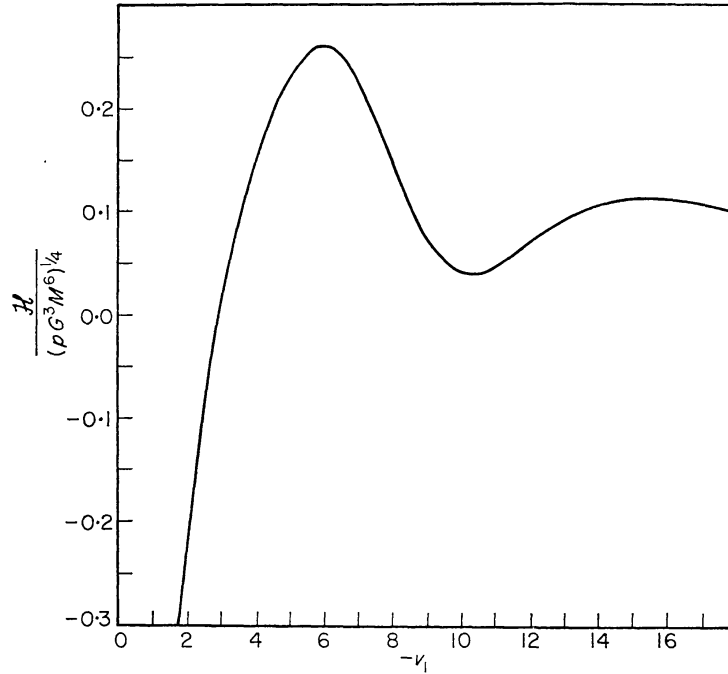
FIG. 4. *Enthalpy–pressure–central concentration relationship.*
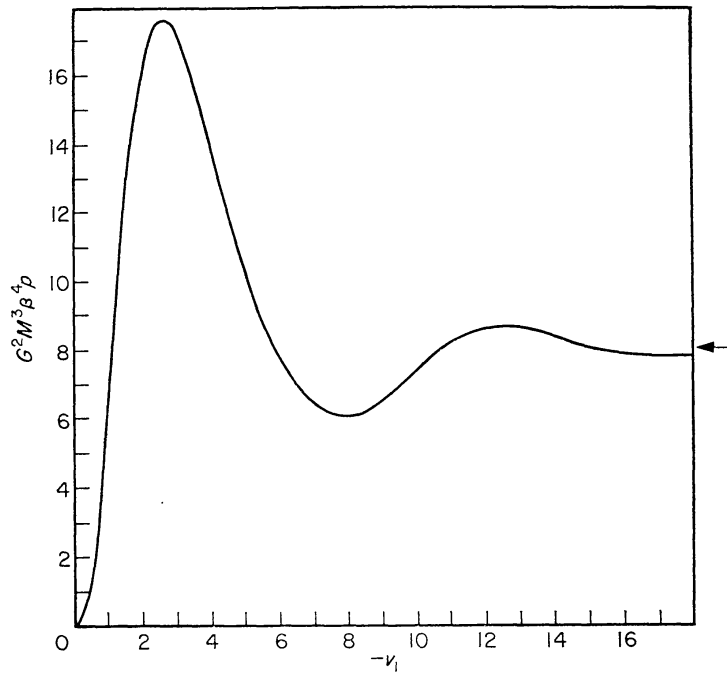
FIG. 5. *Pressure–temperature–density contrast.*

The isotherms are readily calculated since equations (29) and (30) may be rewritten in the forms

$$r_e = GM\beta(-zv_1')^{-1},$$

$$p = (4\pi G^3 M^2 \beta^4)^{-1} (-zv_1')^2 z^2 e^{v_1},$$

while

$$V = \tfrac{4}{3}\pi r_e^3.$$

For an isotherm β is constant and these may be regarded as the parametric equations. The detailed form of the isotherms has already been calculated from such formulae by Bonner, one is plotted here as Fig. 7. All others are scalings of the same curve.

To calculate the adiabats we take equation (27) eliminate β using equation (29), E using (31) and p using (30). We thus obtain

$$\frac{mS}{kM} = -\log\left\{\frac{z^2 e^{v_1}(-zv_1')^{1/2}}{r_e^{3/2}}\right\} + (-zv_1') + \frac{2z^2 e^{v_1}}{(-zv_1')} + \log\left(4\pi G^{3/2}M^{1/2}m\right) - \frac{9}{2}.$$

For any given S this is a relationship between r_e and z; a further relationship for $p(r_e, z)$ is provided by equation (30) with $V = \frac{4}{3}\pi r_e^3$. Together these provide parametric equations for the adiabats which we may now determine using Emden's tables or their equivalent.
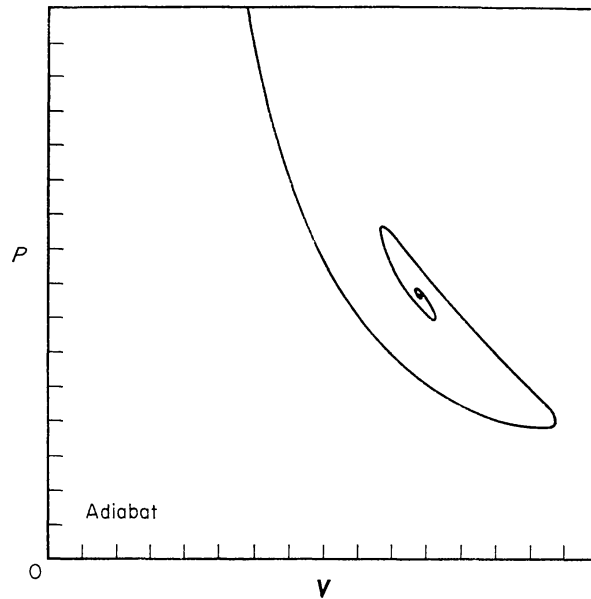

FIG. 6

An adiabat is plotted as Fig. 6. Other adiabats may be obtained by scalings. The reader should note that the breakdown of the adiabat occurs not at small volumes but at large ones. The bounding sphere can be too big for there to be an equilibrium. The physical explanation of this phenomenon is that given in Section 3.

4.5 *Criticism of the statistical calculation.*—By taking Boltzmann's view of entropy rather than Gibbs's we have left out the entropy of the fluctuations about the state considered and have treated the particles as independent so that the two particle distribution functions $f(1, 2) \equiv f(\mathbf{r}_1, \mathbf{c}_1; \mathbf{r}_2, \mathbf{c}_2)$ factored into $f(1, 2) = f(1).f(2)$. Here $f(1) \equiv f(\mathbf{r}_1, \mathbf{c}_1)$ etc. We have thus ignored pairwise correlations. In a normal astrophysical gas this is a good first approximation but the attractive force of gravity clearly helps correlations. In fact had we chosen Gibbs's viewpoint it would have been clear from the start that no full thermodynamic equilibrium was possible at all. Gibbs's canonical approach is to consider every possible state of the whole system giving equal weight to equal volumes
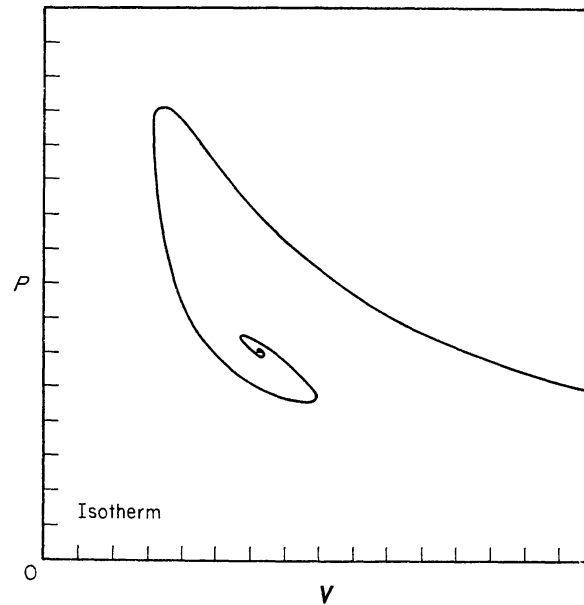
P

Isotherm

O

V

FIG. 7

of the system's $6N$ dimensional phase space apart from a factor exp $\{-\beta'E'\}$. Here E' is the total system energy and β' is chosen so that the average of E' over the ensemble is E. Consideration of simple models shows that the system with a large subset of the particles very closely bound together by gravity and the remainder banging about with the high energy released has a large phase space volume associated with it. So also does the system in which a pair or many pairs of particles are very close together. To obtain any sense from statistical mechanics we must consider systems in which these highly desirable states with infinite weight are unattainable. In practice this is almost the case for real systems because very rare events must be invoked if binaries are to form from the general field. We can therefore consider 'frozen equilibria' in which the number of binaries is unchangeable in the time available. A one particle distribution function is then allowable provided many particle correlations are not pronounced. In a certain rough and ready sense the Gravothermal Catastrophe occurs when such a many particle cooperation just must occur, and we have seen that the statistical method fails to give any answers beyond that point. We have also seen how sub-clustering in the initial conditions can change the whole behaviour even before this. Our other excuse for leaving out high order correlations is that only a fool tries the harder problem when he does not understand the simplest special case.

4.6 *Criticism of stability deductions*. We have argued that we know our sequences are stable at one end, that they do not cross any sequences until they turn-over and therefore that they are stable up to that turnover. We wish here to comment that we do not rigorously know that they do not cross any other sequence. We have calculated *all* the spherical configurations and Appendix II shows that the only stable equilibria are spherical. However these two facts do not prove that our sequence is not crossed by an unstable non-spherical sequence whose only spherical member is at the crossing point. In practice it is hard to think of non-spherical equilibria in this problem but we are led to believe that such exist after the system has become unstable to spherically symmetrical de-

formations. We believe that this point can only be fully cleared up by a stability analysis (21) in the neighbourhood of zero frequency oscillations. Should such a non-spherical unstable sequence cross our sequence before turnover the continuation of our spherical sequence will be unstable.

TABLE I

z	$|v_1|$	ρ_0/ρ_e	Remarks
4·07	1·61	5·0	Turning point of $dM(z)/dz$ (the incremental increase of mass with radius).
4·74	1·93	6·8	Zero of energy for an isolated system of given volume (i.e. the configuration in which the gravitational binding energy just balances the thermal energy).
6·45	2·64	14·1	Minimum of Gibbs free energy for equilibria of systems in contact with a heat bath at constant temperature. Onset of thermal instability at constant pressure (Ebert). Onset of negative★ specific heat at constant pressure, C_p. Maximum of isotherm.
7·25	2·93	18·7	Zero of enthalpy for an isolated system at given pressure.
8·99	3·47	32·2	Minimum of Helmholtz free energy for equilibria of systems in contact with a heat bath at constant temperature. Onset of thermal instability at constant volume. Onset of negative★ specific heat at constant volume, C_v. Vertical tangent to isotherm. Schönberg–Chandrasekhar limit (approx.).
22·5	5·65	287	Minimum temperature for a given energy. Maximum energy for a given temperature.
25·8	5·96	389	Maximum entropy for an isolated equilibrium configuration at given pressure. Least enthalpy for an equilibrium state of given pressure. Onset of dynamical instability in thermally isolated systems at given pressure. Minimum of adiabat.
34·2	6·55	709	Maximum entropy for an isolated equilibrium configuration of given volume (Antonov). Least total energy (greatest binding energy) for an equilibrium state at given volume. Maximum volume for an equilibrium state of given energy. Onset of the gravo-thermal instability in completely isolated systems. Vertical tangent to adiabat.

★ It should be noted that (as described in Section 4.1) the specific heat goes to negative values through *infinity* at these points.

5. *Interesting and critical points.* In Table I we give all the special points found in our discussion. It is imagined that we traverse the sequence in order of increasing density contrast. For the readers convenience we repeat some definitions here.

The radius of the bounding spherical box is r_e

$\dfrac{3}{2\beta}$ is the kinetic energy per unit mass $\tfrac{1}{2}\overline{c^2}$

ρ_0 is the density at the centre

ρ_e is the density at the boundary

$v_1 = \log(\rho_e/\rho_0)$(This is also proportional to the potential measured from zero at the centre.)

z is the dimensionless scaled radius of the box $z = (4\pi G\rho_0\beta)^{1/2}r_e$

$v_1(z)$ is the function found by integrating the isothermal equation.

6. *Astronomical applications*

6.1 *Galaxies.* Throughout this work we have assumed that heat can flow from point to point in our systems. That is we have assumed that the time scale for heat flow is shorter than or of the order of the age of the system. If only interactions between individual stars are considered then the time scale in galaxies is on the contrary much too long, except possibly in the most compact galactic nuclei. On the normal level there is no sensible application to galaxies. However Lynden-Bell (22) recently considered the statistical mechanics of the violent relaxation that occurs when the mean gravity field of the system is unsteady and showed that significant evolution might occur even if these conditions only persisted through the galaxies' birth stages. Furthermore this form of relaxation does not lead to mass segregation and the relaxed states are the same as those of the Fermi–Dirac self-gravitating gas but with a completely different interpretation of the degeneracy. In the relevant limit one recovers the classical isothermal distribution but with no mass segregation. Once this is accepted it is relevant to ask ' Did galaxies in their birth stages undergo the gravo-thermal catastrophe and if so what would they do about it?'

Since galaxies are not contained in hard boxes it is evident that conditions must have been ripe for this event. However, the violent relaxation may not have persisted for long enough for relaxed conditions to be set up throughout a region with a density contrast of 709 to 1. At present this must remain a matter for debate. For our interests sake we shall assume that at least a fraction of galaxies do undergo the gravothermal catastrophe. The centres will then begin to separate into a core—a sort of separate body which might even be called a nucleus. This will cease to shrink when it becomes degenerate in Lynden-Bell's sense. The system will then have a core–halo structure which is an equilibrium of an isothermal Fermi–Dirac gas sphere. These will show a variety of different nuclear concentrations depending on the degeneracy parameter.

It is evident that theory developed along these lines has the chance of making sense of the variety of different galactic nuclei. The first problem to be tackled is obviously the computation of isothermal Fermi–Dirac spheres. This is almost complete. The second is the incorporation of rotation into the study of the gravo-thermal catastrophe.

Two remarks should be added. (i) If in galactic nuclei the star–star relaxation time is short enough then these will in turn relax by the normal process and may undergo the gravothermal catastrophe on their own account. This might be a natural process leading to very high densities in which stars can collide and shed a large proportion of their gas to lead to a dynamic currant bun model. The currants are the cores of the stars, the bun is the gas which is highly turbulent and grows to contain a large fraction of the mass. Such models have been speculatively discussed in the literature in connection with Seyfert nuclei (23), (24) and quasars

(**24**). (ii) It is not clear that violent relaxation is confined to the birth stages of galaxies. Jeans's instabilities might occur persistently in stellar systems and lead to a continuing violent relaxation.

    6.2 *Relevance to the evolution of star clusters by encounters*. Discussions of the evolution of stellar systems due to stellar encounters have emphasized the importance of the escape of stars as the primary cause of continued evolution. Antonov's discussion has shown this to be false. Even if the system is surrounded by a spherical reflecting wall there will be continuing evolution provided that the radius of the sphere is greater than r_c. Once that limit is surpassed the basic urge of the encounters to make the system isothermal is more than counteracted by the heating of the centre due to gravitational contraction. Models based on the hypothesis that the system is close to the isothermal except near the escape energy will therefore breakdown whenever the central concentration becomes large. To demonstrate this still more clearly in models which do not require confining boxes we have calculated the entropies of a sequence of Woolley's models with fixed mass and total energy. Woolley's models are the simplest modification to the isothermal obtained by truncating the distribution function above a certain energy so that

$$f(\epsilon) = \begin{cases} A \exp -\beta\epsilon & -\beta\epsilon > k, \\ 0 & -\beta\epsilon \leqslant k, \end{cases}$$

k, the cut off parameter, will not be confused with Boltzmann's constant. Such models reach an edge at a finite radius. The larger the value of k the larger is that value of r_1 at which the model starts to deviate from the complete isothermal gas sphere. Evolution of the system may be represented by allowing the system to approach the isothermal sphere by gradually increasing its k. In the absence of escape this evolution will be rigorously at constant E and constant M. In the presence of escape E will still be approximately constant since escapers carry away very little energy. M will decrease but it is probable that the main drive of the evolution goes towards increasing k since this involves the more frequent less violent encounters. It is therefore reasonable to consider the idealized evolution at constant E and M to illustrate our point. The evolution proceeds from the low value of k (say $k = 3$ to 5) at which the system is presumed to have been born, and meanwhile the entropy is increased according to the values shown in Table II. However once the cluster has reached $k \sim 8 \cdot 5$ we see that further increase in k would be accompanied by a decrease of entropy. In practice the entropy will inevitably increase so we are forced to deduce that the actual path of evolution departs radically from Woolley's models at this point. It is perhaps worth remarking that actual clusters appear to congregate with values of k somewhat below the critical one.

    These clusters truncated in energy space in fact behave in a similar manner to the isothermal spheres truncated in radius which we have been considering in detail. The maximum of S as a function of k found for Woolley's models corresponds to the maximum of S as a function of v_1 which we showed was associated with the gravothermal catastrophe. It is therefore natural to deduce that the same thing happens. Further evolution ceases to be towards the isothermal gas sphere but instead the temperature contrast between the central nucleus and the outside

TABLE II

$k(= -v_1)$	z	$-v_1'$	$\dfrac{GM\beta}{r_e}(= -zv_1')$	$-\dfrac{\beta E}{M}$	$\dfrac{Er_e}{GM^2}$	$\dfrac{S^*}{-kM}$
3	9·64	0·140	1·35	0·734	0·543	−3·68
4	14·1	0·101	1·43	0·874	0·609	−3·46
5	21·3	0·0645	1·36	0·964	0·694	−3·33
6	34·0	0·0359	1·22	1·008	0·826	−3·23
7	57·4	0·0185	1·06	1·006	0·946	−3·16
8	102·3	0·00914	0·935	0·956	1·022	−3·13
9	183	0·00485	0·886	0·898	1·013	−3·15
10	314	0·00291	0·914	0·858	0·939	−3·21

will increase. Further evolution will probably form a core and an envelope similar to that discussed in the stellar evolution of the red giants.

We emphasize that this is not a peculiar property of Woolley's models by considering the special cases of Michie's models which have been more fully worked out by King (**10**). These again show the phenomenon of a maximum in the binding energy at fixed outer radius; see Fig. 8. The complication of the formula for the
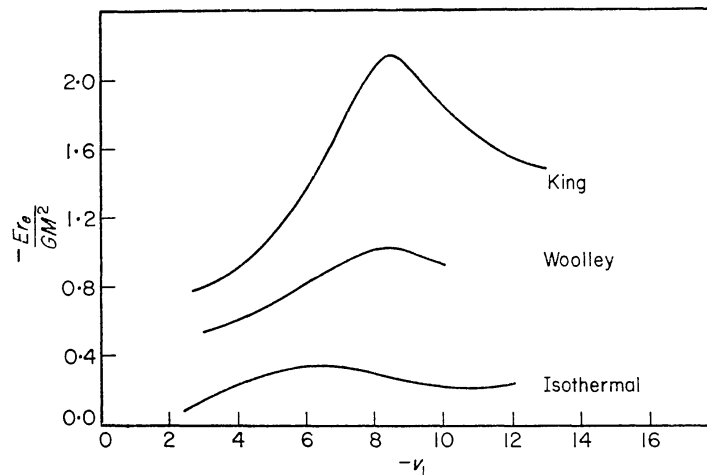

FIG. 8. *Energy–extreme radius against cut off parameter. At constant energy and mass the maximum entropy state corresponds to the maximum.*

entropy deterred us from working it out but in all our other models the maximum in this binding energy occurs at the entropy maximum. We have little doubt that an entropy maximum in the Michie–King sequence occurs at or close to this model.

If this is accepted there becomes an obvious need for models of cluster evolution which are not based on the gradual approach to the isothermal. The basic features of such models must be a core, which evolves towards higher temperatures at a rate determined by its own more rapid relaxation, surrounded by an extensive halo which remains cool. The evolution is similar to the gravitationally contracting stage of a red giant.

6.3 *Analogies with stellar evolution.* It is perhaps worth speculating whether the formation of giants in stellar evolution might not be essentially the same phenomenon as the evolution of a stellar system into a core and a halo. We have not been able to convince ourselves that this is the case but some idea why the systems behave

similarly is as follows. The temperature contrast in a star leads to greater pressure per unit density in the core, but this is to some extent offset by the molecular weight contrast so that the system may simulate an isothermal gas sphere more closely than one might suppose at a first glance. Some might consider that the lack of nuclear energy generation in the dynamics of a star cluster would provide a radical difference in the equilibrium states. However it is salutary to remember that the main properties of the main sequence were deduced without knowledge of the energy generation. It could perhaps be argued that in the less advanced evolutionary stages the main role of energy generation is to slow down the evolution while the energy comes out rather than to alter the evolutionary path. (That is an oversimplification because the change in molecular weight also occurs.)

Star clusters evolve unimpeded by nuclear hold-ups, thus gravitational contraction gives place directly to core formation and the giant phase. Studies of star clusters have the added attraction that one can see the interior!

There are correct analogies between isothermal spheres and stellar evolution. The Schönberg–Chandrasekhar limit (25) is caused by the isothermal core of a star exceeding $z = 9$, which is approximately one of the critical points of Table I.

Royal Greenwich Observatory,
Herstmonceux Castle,
Hailsham,
Sussex.
1967 *August.*

References

(1) Henon, M., 1961. *Ann. Astrophys.*, **24,** 369.
(2) Henon, M., 1965. *Ann. Astrophys.*, **28,** 62.
(3) Aarseth, S. J., 1963. *Mon. Not. R. astr. Soc.*, **126,** 223.
(4) Antonov, V. A., 1962. *Vest. leningr. gos. Univ.*, **7,** 135.
(5) Woolley, R. v. d. R., 1954. *Mon. Not. R. astr. Soc.*, **114,** 191.
(6) Woolley, R. v. d. R., 1956. *Mon. Not. R. astr. Soc.*, **116,** 296.
(7) Woolley, R. v. d. R., 1961. *R. Obs. Bull.*, No. 42.
(8) Michie, R. W., 1963. *Mon. Not. R. astr. Soc.*, **125,** 127.
(9) Michie, R. W. & Bodenheimer, P. H., 1963. *Mon. Not. R. astr. Soc.*, **126,** 269.
(10) King, I. R., 1966. *Astr. J., N.Y.*, **71,** 64.
(11) Ebert, R., 1955. *Z. Astrophys.*, **37,** 216.
(12) Ebert, R., 1957. *Z. Astrophys.*, **42,** 263.
(13) Bonnor, W. B., 1956. *Mon. Not. R. astr. Soc.*, **116,** 351.
(14) McCrea, W. H., 1957. *Mon. Not. R. astr. Soc.*, **117,** 562.
(15) Emden, R., 1907. *Gaskugeln*, Leipzig.
(16) Chandrasekhar, S., 1939. *Stellar Structure*, p. 155, Chicago University Press.
(17) Poincaré, H., 1885. *Acta. Math.*, **7,** 259.
(18) Jeans, J. H., 1919. *Problems in Cosmogony and Stellar Dynamics*, pp. 17–23, Cambridge University Press.
(19) Jeans, J. H., 1928. *Astronomy and Cosmogony*, Chap. 7, Cambridge University Press.
(20) Lyttleton, R. A., 1953. *Stability of Rotating Liquid Masses*, pp. 6–15, Cambridge University Press.

(21) Lynden-Bell, D., 1966. *I.A.U. Symposium No.* 25 (1964), p. 78, Academic Press, New York.
(22) Lynden-Bell, D., 1967. *Mon. Not. R. astr. Soc.,* **136,** 101.
(23) Spitzer, L. & Saslaw, W. C., 1966. *Astrophys. J.,* **143,** 400.
(24) Spitzer, L. & Stone, M. E., 1967. *Astrophys. J.,* **147,** 519.
(25) Schönberg, M. & Chandrasekhar, S., 1942. *Astrophys. J.,* **96,** 161.

APPENDIX I

Identification of β' with $1/kT$ and S with thermodynamic entropy

From equations (31) and (30)

$$E = -\frac{GM^2}{r_e}\, q(z),$$

$$p = \frac{GM^2}{4\pi r_e^4}\, g(z)$$

where

$$g(z) \equiv \frac{z^2 e^{v_1}}{(-zv_1')^2} \text{ and } q(z) = \frac{3}{2(-zv_1')} - g(z). \tag{A.1}$$

The heat dQ is given by

$$dQ = dE + p\,dV = \frac{GM^2}{r_e^2}\,[g(z)+q(z)]\,dr_e - \frac{GM^2}{r_e}\,q'(z)\,dz.$$

We rewrite this

$$\frac{dQ}{\frac{2}{3}\dfrac{GM^2}{r_e}\,[g(z)+q(z)]} = \frac{3}{2}\frac{dr_e}{r_e} - \frac{\frac{3}{2}q'(z)}{g(z)+q(z)}\,dz. \tag{A.2}$$

But $\frac{2}{3}[g(z)+q'z)] = [-zv_1']^{-1}$ and from equation (29)

$$\beta = \left[\frac{GM}{r_e}\right]^{-1}(-zv_1')$$

hence equation (A.2) may be written

$$\beta\,dQ = M\,d\left[\tfrac{1}{2}\log V - \tfrac{3}{2}\int\frac{q'(z)}{g+q}\,dz\right] = M\,d\,[\tfrac{1}{2}\log V - I]. \tag{A.3}$$

β is thus an integrating factor for dQ. After a lengthy calculation using the definitions (A.1) and the fundamental equation (15) written in terms of $\log z$ instead of z we find

$$I \equiv \int^z\frac{q'(z)}{\frac{2}{3}(g+q)}\,dz = 2\log z + \tfrac{1}{2}\log(-zv_1') + 2q(-zv_1') - (zv_1') + v_1$$

Comparing this with equation (32) we see that $\tfrac{1}{2}\log V - I$ is the quantity formerly called mS/kM, equation (A.3) may therefore be written $k\beta'dQ = dS$. β' may be identified with $(kT)^{-1}$ and S with thermodynamic entropy. To ensure uniqueness of this identification it is necessary that S should be additive. In one sense this follows directly from the definition (1) which may be used to define an entropy density. However it is not possible to put two gravitating systems side by side

33

without them affecting one another so neither energy nor our entropy S is a simple extensive parameter in the normal thermodynamic sense (i.e. at constant β' and M/V they are not proportional to M).

APPENDIX II

Antonov's proof of spherical symmetry

We have shown in Section 4.3 that the equilibrium states at constant volume can be considered either as states of maximum entropy for given energy or as states of minimum energy for given entropy. Whereas we have formerly employed the first of these to discuss equilibria it is convenient here to use the second. Suppose we have a non-spherically symmetrical system of density $\rho(x, y, z)$. Now imagine an inhomogeneous incompressible fluid also of density ρ. We can displace the elements of fluid without changing their density so that the fluid becomes spherically symmetrical with density monotonically decreasing outwards. During the displacement the entropy of each element of fluid its mass and its kinetic energy remain unchanged. However the potential energy of the whole system has been decreased (since heavy liquid sinks spontaneously). Thus the systems of locally minimal energy for given entropy are spherical. The systems of locally maximal entropy for given energy are the same, so they are likewise spherical.

APPENDIX III

Antonov's proof that global entropy maxima do not exist

Consider the following non-equilibrium distribution. Let mass αM be uniformly distributed inside a sphere of radius r_1. Let the velocities have an upper limit c_1 but let all velocities less than c_1 be equally likely. Let the remainder of the system of mass $(1-\alpha)M$ be distributed in another distant sphere of radius r_2 with an analogous distribution with speed limit c_2. Let the distance between the spheres be r_{12}.

The distributions functions are

$$f_1 = \frac{\alpha M}{m \frac{4}{3}\pi r_1^3 \frac{4}{3}\pi c_1^3} = \frac{\alpha M}{m \frac{16}{9}\pi^2 r_1^3 c_1^3},$$

$$f_2 = \frac{(1-\alpha)M}{m \frac{16}{9}\pi^2 r_2^3 c_2^3}.$$

The entropy is

$$S = -k \frac{\alpha M}{m} \log f_1 - k \frac{(1-\alpha)M}{m} \log f_2$$

$$= -\frac{kM}{m} [\alpha \log \alpha + (1-\alpha) \log (1-\alpha)]$$

$$+ \frac{3kM}{m} [(1-\alpha) \log c_2 r_2 + \alpha \log c_1 r_1] - \frac{kM}{m} \log \frac{9M}{16\pi^2 m}. \tag{A.4}$$

The total energy is

$$E = -\tfrac{3}{5} GM^2 \left[\frac{\alpha^2}{r_1} + \frac{(1-\alpha)^2}{r_2} + \tfrac{5}{3} \frac{\alpha(1-\alpha)}{r_{12}} \right] + \tfrac{3}{10} M \left[\alpha c_1{}^2 + (1-\alpha)c_2{}^2 \right]. \quad (A.5)$$

The aim is to make S large by keeping the $(1-\alpha) \log c_2 r_2$ term bounded and making the $\alpha \log c_1 r_1$ term tend to infinity. To this end we fix

$$(1-\alpha) \log c_2 r_2 = -L = \text{const}$$

and we keep c_2 and r_1 constant also. To satisfy equation (A.5) we choose

$$c_1{}^2 = \frac{1}{\alpha} \left[\frac{10}{3M} \left\{ E + \frac{G\alpha(1-\alpha)M^2}{r_{12}} \right\} + \frac{2G\alpha^2 M}{r_1} - (1-\alpha)c_2{}^2 + \frac{2GL^2 M}{r_2[\log(c_2 r_2)]^2} \right]. \quad (A.6)$$

Now let $r_2 \to 0$ then by equation (A.5) $\alpha \to 1$.

From equation (A.6) $c_1 \to \infty$ and from equation (A.4)

$$S \to 0 + 0 - \frac{3kM}{m} L + \infty + \text{const} = \infty.$$

It is perhaps worth noting that the departure from spherical symmetry assumed in this proof is unnecessary since a similar proof holds if the first system lies between spheres concentric with the second system.

APPENDIX IV

Gravitating hard spheres and the non-relativistically degenerate problem

It is perhaps of interest to note that gravitating hard spheres always have a true maximum entropy equilibrium state. When the system approaches the gravothermal catastrophe the system undergoes a phase transition in which a core of hard spheres in contact with one another is formed; outside this core the system obeys the isothermal equation but now takes up one of the 'other' solutions of type (iii). The central support provided by the close packed hard spheres takes the place of the support provided by the unphysical repulsive mass at the origin.

Very similar circumstances prevail with the non-relativistically degenerate spheres. In this case the central part instead of going rock hard becomes degenerate and is thus a polytrope of index 3/2, hard enough to resist gravity. Again outside this degenerate core the system lies on the 'other' solutions of the isothermal sphere.

It seems that in both these systems a phase transition is occurring which replaces the catastrophe of the classical point-particle model.

APPENDIX V

Calculation of the energy and entropy of Woolley's truncated isothermal spheres

The distribution function for these models is

$$f = \begin{cases} A \exp(-\beta\epsilon) & \beta(\epsilon + \psi_0) < k, \\ 0 & \beta(\epsilon + \psi_0) > k. \end{cases}$$

This leads to a density

$$\rho = \begin{cases} \rho_0 e^{v_1} \dfrac{\mathrm{erf}_2 \, (k+v_1)^{1/2}}{\mathrm{erf}_2 \, k^{1/2}} & -v_1 < k, \\[2mm] 0 & -v_1 > k \end{cases}$$

where v_1 is defined in the same way as for isothermal models (equation (13)). Defining $r_1 = (4\pi G \, \rho_0 \beta)^{1/2} r$ Poisson's equation becomes

$$\frac{1}{r_1^2} \frac{d}{dr_1} \left(r_1^2 \frac{dv_1}{dr_1} \right) = \begin{cases} -e^{v_1} \dfrac{\mathrm{erf}_2 \, (k+v_1)^{1/2}}{\mathrm{erf}_2 \, k^{1/2}} & -v_1 < k, \\[2mm] 0 & -v_1 > k. \end{cases}$$

This is solved numerically subject to the conditions

$$v_1 = \frac{dv_1}{dr_1} = 0$$

at $r_1 = 0$. The total potential energy may be found as follows

$$\mathcal{U} = -\tfrac{1}{2} \int \rho \psi \, d^3r = \frac{1}{8\pi G} \int \psi \nabla^2 \psi \, d^3r$$

$$= -\frac{1}{8\pi G} \int (\nabla \psi)^2 \, d^3r + \frac{1}{8\pi G} \int \psi \nabla \psi . d\mathbf{S}$$

where $d\mathbf{S}$ is an element of surface area of the body $(4\pi r_e^2)$. In terms of $v_1(r_1)$ the potential may be written

$$\mathcal{U} = \frac{-1}{2G\beta^2(4\pi G \rho_0 \beta)^{1/2}} \int_0^z (r_1 v_1')^2 dr_1 - \frac{1}{2} \frac{GM^2}{r_e}$$

where z is the value of r_1 at the surface.

Now

$$-\frac{GM}{r_e^2} = \left(\frac{d\psi}{dr} \right)_{r_e} \quad \text{so} \quad \frac{GM\beta}{r_e} = -z v_1'.$$

Hence

$$-\frac{\beta E}{M} = -\frac{\beta \mathcal{U}}{2M} = \frac{\int_0^z (r_1 v_1')^2 \, dr_1}{4z \, (-z v_1')} + \frac{1}{4}(-z v_1'). \qquad (\mathrm{A}.7)$$

The right hand side may be computed numerically from the solutions to equation (15). This must be done for each value of the cut-off k.

To calculate the entropy we note using equation (25) for $\log f$

$$\frac{S}{-k} = \int f \log f \, d^6\tau = -\beta \mathcal{T} - 2\beta \mathcal{U} + M \log A.$$

Using the Virial theorem this may be written

$$\frac{S}{-kM} = -3\beta \frac{E}{M} + \log A.$$

One may show that

$$\rho_0 = A \left(\frac{2\pi}{\beta} \right)^{3/2} \exp(\beta \psi_0) \, \mathrm{erf}_2 \, k^{1/2}$$

and that

$$\beta \left(\psi_0 - \frac{GM}{r_e} \right) = -v_1(z),$$

while

and

$$4\pi G \, \rho_0 \beta = (z/r_e)^2$$

and

$$\beta = \left(\frac{r_e}{GM} \right)(-zv_1')$$

and

$$V = \tfrac{4}{3}\pi r_e{}^3 = \tfrac{4}{3}\pi \frac{\left(-\beta \dfrac{E}{M} \right)^3}{(-zv_1')^3} \left(\frac{GM^2}{-E} \right)^3.$$

From these equations A may be determined to give the following forms for the entropy

$$\frac{S}{-kM} = -3\beta \frac{E}{M} - \tfrac{1}{2} \log V + \log \left[z^2 (-zv_1')^{1/2} \right] - (-zv_1')$$

$$- \log (\mathrm{erf}_2 \, k^{1/2}) + v_1(z) - \tfrac{1}{2} \log (96\pi^4 G^3 M)$$

or eliminating V and putting

$$\frac{S^*}{-kM} = -3\beta \frac{E}{M} - \tfrac{3}{2} \log \left(-\beta \frac{E}{M} \right) + \log \left[z^2 (-zv_1')^2 \right] + v_1(z)$$

$$- (-zv_1') - \log (\mathrm{erf}_2 \, k^{1/2})$$

we have

$$\frac{S}{-kM} = \frac{S^*}{-kM} - \tfrac{1}{2} \log \left[128 \, \pi^5 G^6 M^8 / (-E^3) \right].$$

$\beta E/M$ is the function of z given in equation (A.7) while the last term is constant and may be omitted for a discussion of our sequence of models. The relevant integrated properties of Woolley's sequences are given in Table II.